Randomly oriented ZnO nanowires grown on amorphous SiO$_2$ by metal-catalyzed vapour deposition

D. Comedi [a,b,*], M. Tirado [c], C. Zapata [a], S.P. Heluani [a], M. Villafuerte [a,b], P.K. Mohseni [d], R.R. LaPierre [d]

[a] Laboratorio de Física del Sólido (LAFISO), Dep. Física, FACET, Universidad Nacional de Tucumán, Avda. Independencia 1800, 4000 Tucumán, Argentina
[b] Consejo Nacional de Investigaciones Científicas y Técnicas, Argentina
[c] Laboratorio de Propiedades Dieléctricas de la Materia, Dep. Física, FACET, UNT, Avda. Independencia 1800, 4000 Tucumán, Argentina
[d] Dep. Eng. Physics, McMaster University, 1280 Main St. W, Hamilton L8S 4L7 ON Canada

ABSTRACT

Randomly oriented ZnO nanowire (NW) networks have been grown on thermal SiO$_2$ substrates by the simple carbothermal reaction-assisted thermal evaporation of ZnO. One-dimensional growth was achieved with the aid of Au nanocluster catalysts dispersed on the substrates. The structures were studied by scanning electron microscopy, energy dispersive X-ray analysis, and X-ray absorption spectroscopy. The NW diameters and lengths were found to strongly depend on the substrate temperature (T_S) and to be in the 5–10 nm and 40–110 nm ranges for T_S = 520 °C, and in the 50–80 nm and 1–3 μm ranges for T_S = 700 °C, respectively. The growth regime was characterized by comparing the NW structures obtained on SiO$_2$ with those grown in the same deposition run on (1 0 0) Si substrates also covered with the Au catalyst. The NW structure prepared at 700 °C behaves as a dense NW network with net electrical conductance and persistent photoconductance. These results suggest a method to deposit size-controlled ZnO NW networks on insulating cost-effective substrates with important potential applications as in chemical sensors and solar cells.

© 2009 Elsevier B.V. All rights reserved.

1. Introduction

Semiconductor nanowires (NWs) have been proposed as basic "building blocks" in a variety of devices in many applications, such as photonics, electronics and chemical sensing [1]. For instance, the large surface area offered by NWs is very attractive for solar cells where high surface chemical sensitivity and efficient light trapping and absorption are needed. Most studies report on efforts to grow vertically aligned ZnO NW arrays on various substrates (notably on Si [2,3] and saphire [4,5]). An important requirement for cost-effectiveness is the possibility of growing NWs on inexpensive and transparent substrates, such as glass [6]. Growth of vertically aligned ZnO NWs on a vacuum deposited SiO$_2$ film on a Si substrate has been reported [7]. Here, NW alignment was achieved by fabricating a thin seed ZnO layer on the SiO$_2$ film prior to NW growth. However, an interesting and potentially useful assembly is in the form of ramdom networks of interconnected NWs on insulating substrates. A printing technique has been reported where vertically aligned ZnO NWs are first deposited on metal-catalyzed

Si and then detached from the growth substrate by pressing it onto a receiving substrate where the NW network forms [8]. In this work, we report on the direct growth of randomly oriented ZnO NW networks on thermal SiO$_2$ layers on Si using the metal catalysis method. The electrical properties of the NW networks can be easily tested right on the insulating SiO$_2$/Si growth substrates and exhibit macroscopic conduction and photoconduction with potential sensor, photovoltaic and other optoelectronic applications

2. Experimental details

Substrates were amorphous SiO$_2$ layers (0.5 μm-thick, grown on Si by thermal oxidation) where a thin (5 nm) Au layer had been deposited and annealed at 500 °C for 15 min to produce nanometer-sized Au clusters on it [9]. The Au nanoclusters are known to act as metal catalysts for one-dimensional growth for various systems [1]. Si (1 0 0) substrates with identically prepared Au nanoclusters were also used as a crystalline substrate reference. NW growths were performed at the LAFISO vapour-transport system, which consists of a 1⅜″ diameter, 1 m long quartz tube placed within a 0.6 m length tubular furnace. One side of the quartz tube is seal-connected through a vacuum valve to a rotary pump while its other side to a high purity (99.999%) Ar line made of a 1/4″ diameter stainless steel tube. An alumina crucible containing ZnO and graphite powders (2:1 volume ratio) was placed inside the quartz tube at a position corresponding to the furnace center. Pairs of Si (1 0 0) and SiO$_2$/Si substrate pieces were placed parallel to the tube axis facing upwards at two different distances downstream the tube (16 and 19 cm from the furnace center), which resulted in two different substrate temperatures due to the natural temperature gradient profile along the tube. After Ar-purging and evacuating the quartz tube to ∼80 mTorr, a steady Ar flow was established by controlling the pumping speed
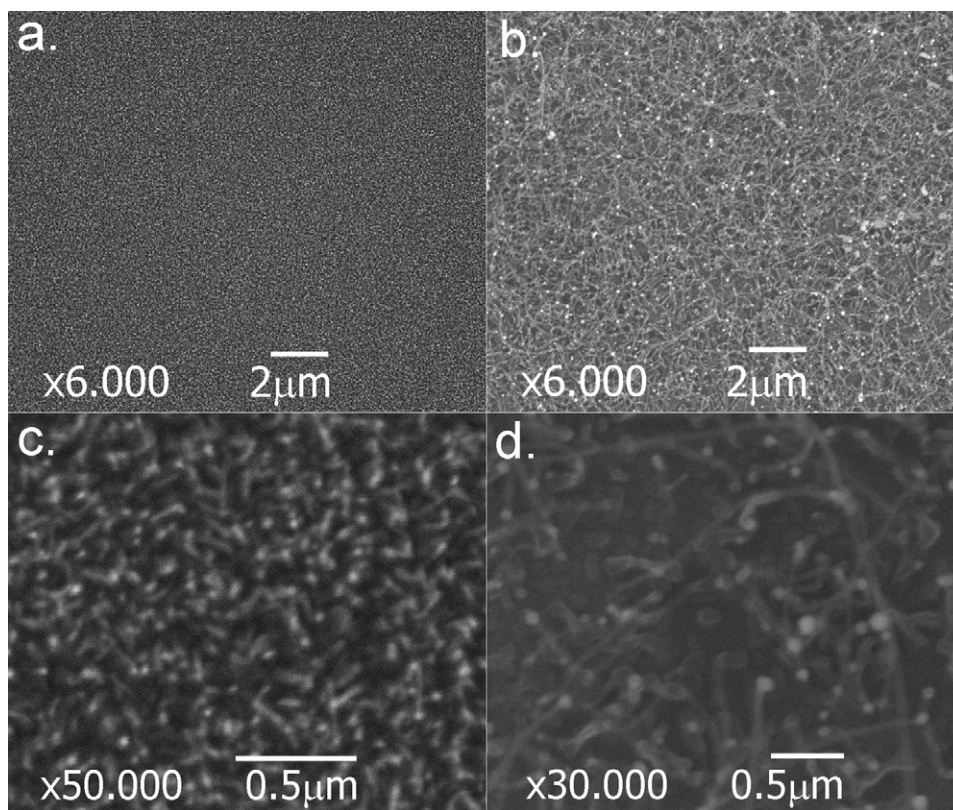
Fig. 1. SEM images under different magnifications of ZnO NWs deposited on Au catalyst/SiO$_2$ substrate. Left (a and c) correspond to T_S = 520 °C and right (b and d) to T_S = 700 °C.

through the vacuum valve, raising the pressure in the tube to about 200 mTorr. The furnace temperature at its center was then ramped to T_{cruc} = 1100 °C at 25 °C/min, maintained constant at 1100 °C for 1 h and then naturally cooled down to room temperature. Under these conditions, substrate temperatures during depositions at T_{cruc} = 1100 °C were determined to be T_s = 520 °C and 700 °C. Scanning electron microscopy (SEM) images were obtained with a JSM 6480 LV system in Argentina and with a JEOL JSM-7000F field emission SEM at McMaster. Energy dispersive X-ray analysis (EDX) spectra were obtained at McMaster with electron accelerating voltage of 10 keV using an INCA system and a Si detector. One of the samples was examined by X-ray absorption measurements at the Brazilian synchrotron laboratory (LNLS) in order to determine its chemical state. The electrical conductance of NW networks was determined by applying a DC bias between two Ag contacts formed on the top of the network (separation of 1 mm) and measuring the current. Photoconductance was assessed by illuminating the region between contacts with UV light (3.1 eV) and monitoring changes in the electrical current.

3. Results

After the depositions, a white powder partially covering both types of substrates is typically seen. Fig. 1(a–d) shows SEM images for deposits on SiO$_2$ at 520 and 700 °C, at two different magnifications for each temperature. The formation of NWs can be seen at both temperatures.

A close look at the NWs reveals that they exhibit bright spots at their tips. For 520 °C the diameters of the wires are around 5–10 nm and their lengths 50–100 nm. For T_s = 700 °C, the NWs are significantly larger (diameters between 50 and 80 nm and lengths between 1 and 3 μm), and are merged together into a dense network. Analysis of their directions reveals no preferential alignment, i.e. they are randomly oriented.

EDX spectra show the presence of Zn, O, C and Au. Fig. 2(a) shows a typical EDX spectrum for the sample deposited at 520 °C with the electron beam focused close to a single NW tip (at the center of the SEM picture shown in Fig. 2(b)). The resolution of the instrument does not permit to obtain a spectrum from isolated tips; however it is clear from the present analysis that they contain mainly Au.

The signal due to O comes from both the SiO$_2$ substrate and from the ZnO NW, while the Au signal is due to the small bright spot at the NW tip. Also, small C content can be detected, which originates from the graphite reactant.

This kind of structure closely resembles the metal cluster-led growth behaviour that is typical for vapour–liquid–solid (VLS) [10] or vapour–solid–solid (VSS) [1] mechanisms. Furthermore, we have confirmed that depositions under similar conditions on SiO$_2$ substrates without the Au catalyst do not produce NW networks, but sporadic nanometer-sized, irregularly shaped ZnO formations.

We have used X-ray absorption spectroscopies (near edge-XANES and extended fine structure-EXAFS) to determine the prevailing atomic configurations within the nanostructures obtained. Fig. 3 shows the XANES spectrum obtained for the sample deposited at 700 °C, as compared to spectra from pure ZnO and metallic Zn reference samples. The sample spectrum resembles closely that of the ZnO, albeit slightly shifted to the low energy side, indicating the presence of a small volume fraction of substoichiometric oxide (i.e ZnO$_x$ with $x < 1$) and probably also some metallic Zn. The EXAFS oscillation patterns shown in the insert confirm that the material is essentially ZnO with small substoichiometric particles or domains.

Interestingly, the growth mechanism for the same deposition conditions is completely different on crystalline Si substrates. Fig. 4 shows ZnO structures deposited on a Au/Si (1 0 0) substrate placed just beside the Au/SiO$_2$ substrate at 520 °C in the same growth run. It can be seen that in this case hexagonal-shaped nanorods grow epitaxially aligned with the Si [1 0 0] direction, but also with other few preferred directions. These nanorods achieve much larger diameters and shorter lengths than the NWs grown on SiO$_2$, and also span a wider diameter distribution that goes from about 10 to 100 nm. The hexagonal shape is typical for growth along the c-direction of wurtzite ZnO. At 700 °C, the ZnO crystals are much larger (several hundreds of nm) and merge into a continous 2D nanocrystalline layer (not shown here).
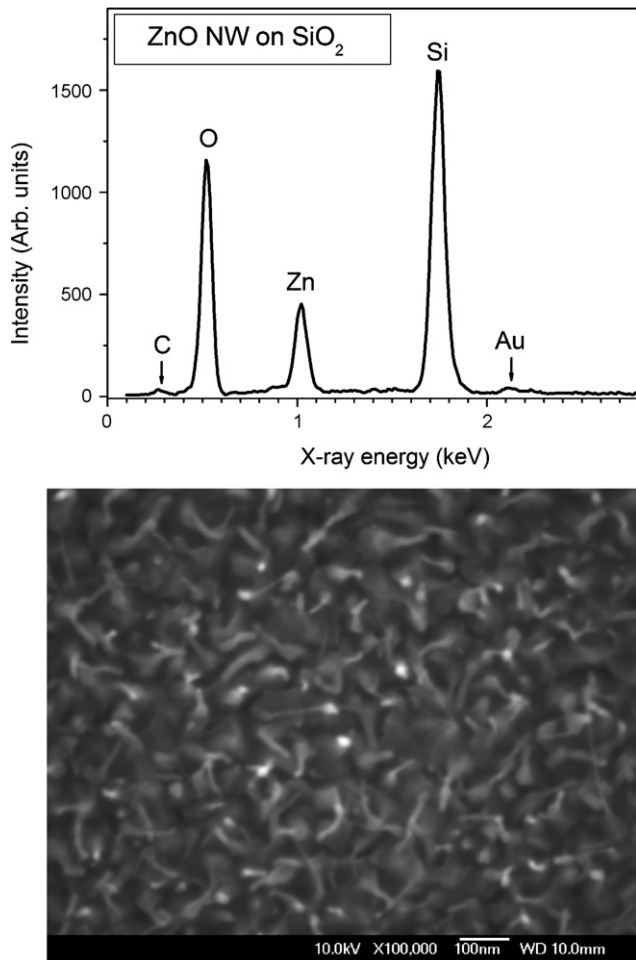
Fig. 2. (Top) EDX spectrum of ZnO NW with the electron beam focused at the tip region of a NW (center of the SEM picture shown in the bottom figure).

The as-deposited, randomly oriented NWs behave as a three-dimensional random network of wires whose density ($\sim$2–4 NWs/μm^3) is above the percolation threshold (roughly speaking, the average distance between NWs is smaller than the average NW length [11]). The network exhibits slightly nonlin-
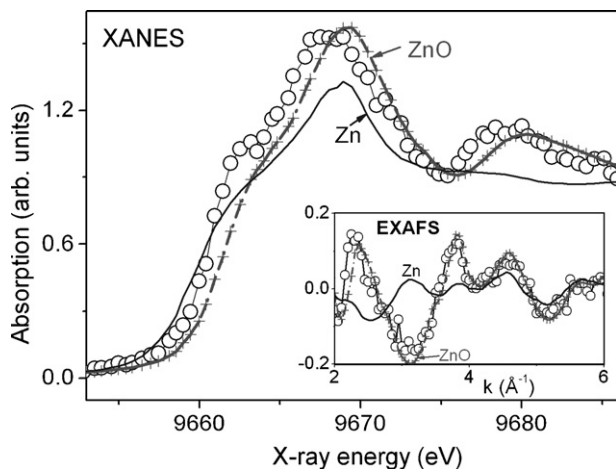

Fig. 4. ZnO structures grown on a (1 0 0) Si substrate dispersed with Au catalysts under the same deposition conditions as the sample shown in Fig. 1(a and c).

ear *I–V* characteristics with a resistance of about 40 kΩ, and its conductance increases with increasing sample temperature (i.e., semiconducting behaviour). The *I–V* characteristics and the current as a function of UV illumination and time are shown in Fig. 5. The incident photon energy (3.1 eV) is slightly lower than the typical ZnO band gap of $\approx$3.3 eV, hence the light is expected to be absorbed weakly at each NW layer and to illuminate all through the NW network down to the network/substrate interface.

4. Discussion

At 1100 °C, the sublimation rate of pure ZnO is negligible, however ZnO grains in contact with graphite particles react by the well-known carbothermal reaction leading to Zn, ZnO$_x$ (x < 1) and CO$_2$ species [12]. Immediate sublimation of metallic Zn and ZnO$_x$ produces Zn and Zn suboxide vapours, which are transported by the Ar flow or diffuse towards cooler regions in the furnace, where the substrates are held. These vapour species must be oxidized to produce ZnO; this must occur at the substrate where they land. From the XANES/EXAFS data (Fig. 3), we see that the oxidation rate is sufficient to produce ZnO, albeit some under coordinated Zn remains in the form of O vacancies or metallic Zn inclusions.

Fig. 3. X-ray absorption near the Zn K-edge (XANES) spectrum obtained for a ZnO NW sample deposited at T_s = 700 °C (circles). The reference spectra for a ZnO crystal (crosses and dash-dot line) and metallic Zn (solid line) are also shown for comparison. Inset: Corresponding extended X-ray absorption fine structure (EXAFS) spectrum, together with the corresponding ZnO and Zn reference spectra.
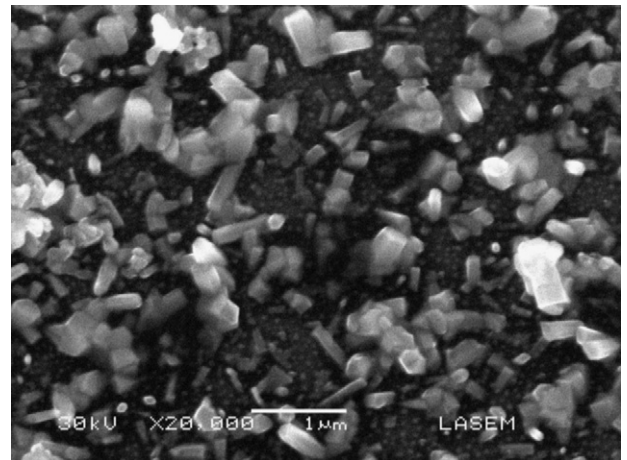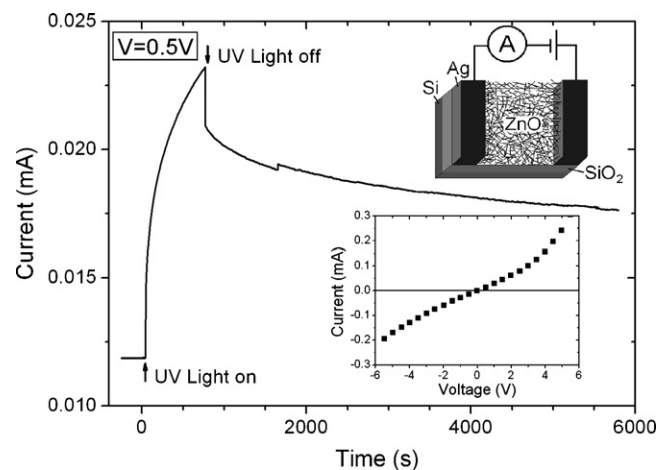

Fig. 5. Electrical current as a function of time for ZnO NW network obtained in this work, measured at a voltage of 0.5 V with and without UV light (3.1 eV photon energy) illumination. Insets: contact configuration (top) and current as a function of voltage without illumination (bottom).

The results on different substrates demonstrate that the substrate material and structure play a very important role in the determination of the reaction kinetics that lead to the formation of the ZnO nanostructures. On Si (1 0 0), the size distribution of formations is wider than for the SiO_2 substrate, which could be due to a corresponding wider size distribution of Au nanoclusters expected from the larger surface energy of the crystalline material than that of the oxide [9]. In addition, ZnO crystallite nucleation and relatively ordered growth seem to be promoted on Si (1 0 0) by epitaxy related to crystalline Si directions. On amorphous SiO_2, in contrast, the lack of a crystalline substrate inhibits epitaxial effects and the Au-catalyzed one-dimensional growth in random directions prevails. In both cases, mechanisms such as VLS or VSS are expected to play an important role [1,13]. In the VLS mechanism, the Zn atoms landing at the Au particles form a supersaturated ZnAu eutectic melt where Zn reacting with O atoms precipitate towards the substrate, inducing one-dimensional ZnO growth. In the VSS mechanism, the Au/Zn nanoparticle is not in the liquid state, and growth may be catalyzed by enhanced diffusion of ZnO at the metal surface towards the metal/substrate or metal/nanowire interface.

In either of the above described mechanisms, it is clear that the substrate temperature will play a very important role by increasing the diffusion of adsorbed species, the Zn oxidation rates involved in the formation of ZnO, and the average size of the Au clusters [9]. All of these should contribute to an increase of the NW sizes with increasing T_S, as indeed observed in the present study. It is, however, interesting to note that others have found an opposite trend in a very similar vapour-transport/Au catalyst system as the one used here (see for instance [4]). In Ref. [4], increasing T_S led to lower ZnO NW diameters, probably because of the thermally induced re-evaporation of deposited ZnO species from NW walls. The most significant difference with our experiment seems to be the larger pressure range explored in [4] ($P > 750$ mTorr), which is expected to significantly lower the diffusivity of growth precursors through the Ar gas [14]. In our case diffusion is certainly a factor due to the low pressure used (200 mTorr) and we observe, in fact, some ZnO growth upstream the quartz tube walls, i.e., not only in the direction of the Ar flow. Hence, it is probable that in the prevailing diffusive regime, the re-evaporation of ZnO species is overcompensated by the incoming diffusive precursor flux, and hence the NW diameters increase with increasing T_S due to the increasing oxidation and various diffusion rates.

The conductance of the dense ZnO NW network (see Figs. 1 and 5) is determined by the conductivity of each NW, the NW–NW connectivity and the NW density and it should be useful for sensor applications. The conductivity of each NW, in turn, is probably fixed by the O vacancy and Zn interstitial densities because, as shown very recently, these defects may form n-type dopant complexes in ZnO [15]. Another possibility could be surface conduction through the NW walls [16]. Our networks show quasi-persistent photoconductivity as has been observed in ZnO thin films and, very recently, also in other ZnO NWs [17]. This effect has been attributed to the slow release of charge carriers from band gap traps. Further experiments are in progress to study the role of ZnO NW structure and stoichiometry on the electrical and photo-electrical characteristics of our ZnO NW networks and to assess their potential applications in sensors and solar cells.

5. Conclusion

Randomly oriented ZnO NW networks have been grown on thermal SiO_2 substrates by the simple carbothermal reaction-assisted thermal evaporation of ZnO combined with the metal catalysis method. The NW diameters and lengths are in the 5–10 nm and 50–100 nm ranges for $T_S = 520\,°C$, and in the 50–80 nm and 1–3 μm ranges for $T_S = 700\,°C$, respectively. The growth regime was characterized by comparing the NW structures obtained on SiO_2 with those grown in the same growth run on (1 0 0) Si also covered with the Au catalyst. These results suggest the possibility of controlling the NW size via T_S in NW random networks on insulating cost-effective substrates. The NW networks obtained at 700 °C show considerable conductance and photoconductance. These properties, in addition to their high surface area to volume ratio, make these networks promising candidates for chemical sensors and solar cells.

References

[1] N. Wang, Y. Cai, R.Q. Zhang, Mater. Sci. Eng. R 60 (2008) 1.
[2] G. Zhang, A. Nakamura, T. Aoki, J. Temmyo, Y. Matsui, Appl. Phys. Lett. 89 (2006) 113112.
[3] F. Fang, D.X. Zhao, J.Y. Zhang, D.Z. Shen, Y.M. Lu, X.W. Fan, B.H. Li, X.H. Wang, Nanotechnology 18 (2007) 235604.
[4] S.H. Dalal, D.L. Baptista, K.B.K. Teo, R.G. Lacerda, D.A. Jefferson, W.I. Milne, Nanotechnology 17 (2006) 4811.
[5] S.T. Ho, C.Y. Wang, H.L. Liu, H.N. Lin, Chem. Phys. Lett. 463 (2008) 141.
[6] R. Könenkamp, R.C. Word, C. Schlegel, Appl. Phys. Lett. 85 (2004) 6004.
[7] S.N. Cha, B.G. Song, J.E. Jang, J.E. Jung, I.T. Han, J.H. Ha, J.P. Hong, D.J. Kang, J.M. Kim, Nanotechnology 19 (2008) 235601.
[8] H.E. Unalan, et al., Appl. Phys. Lett. 94 (2009) 163501.
[9] M.C. Plante, J. Garrett, S.C. Ghosh, P. Kruse, H. Schriemer, T. Hall, R.R. LaPierre, Appl. Surf. Sci. 253 (2006) 2348.
[10] R.S. Wagner, W.C. Ellis, Appl. Phys. Lett. 4 (1964) 89.
[11] S. Kumar, J.Y. Murthy, M.A. Alam, Phys. Rev. Lett. 95 (2005) 066802.
[12] B.D. Yao, Y.F. Chan, N. Wang, Appl. Phys. Lett. 81 (2002) 757.
[13] S.Y. Li, P. Lin, C.Y. Lee, T.Y. Tseng, J. Appl. Phys. 95 (2004) 3711.
[14] A. Colli, A. Fasoli, S. Hofmann, C. Ducati, J. Robertson, A.C. Ferrari, Nanotechnology 17 (2006) 1046.
[15] Y.S. Kim, C.H. Park, Phys. Rev. Lett. 102 (2009) 086403.
[16] Y.W. Heo, L.C. Tien, D.P. Norton, B.S. Kang, F. Ren, B.P. Gila, S.J. Pearton, Appl. Phys. Lett. 85 (2004) 2002.
[17] Z.-M. Liao, Y. Lu, J. Xu, J.-M. Zhang, D.-P. Yu, Appl. Phys. A 95 (2009) 363.